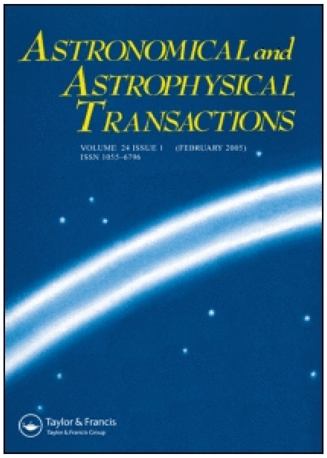

Astronomical & Astrophysical Transactions

The Journal of the Eurasian Astronomical Society

Publication details, including instructions for authors and subscription information:
http://www.informaworld.com/smpp/title~content=t713453505

Model calculations of matter outflow from active galactic nuclei

E. Y. Vilkoviskij [a]; R. V. E. Lovelace [b]; M. M. Romanova [b]; L. A. Pavlova [a]; S. N. Yefimov [a]; E. B. Baturina [a]

[a] Observatory, Fesenkov Astrophysical Institute, Almaty, Kazakhstan
[b] Cornell University, Ithaca, New York, USA

Online Publication Date: 01 August 2005

To cite this Article: Vilkoviskij, E. Y., Lovelace, R. V. E., Romanova, M. M., Pavlova, L. A., Yefimov, S. N. and Baturina, E. B. (2005) 'Model calculations of matter outflow from active galactic nuclei', Astronomical & Astrophysical Transactions, 24:4, 343 - 353

To link to this article: DOI: 10.1080/10556790500487122
URL: http://dx.doi.org/10.1080/10556790500487122

Astronomical and Astrophysical Transactions
Vol. 24, No. 4, August 2005, 343–357

Model calculations of matter outflow from active galactic nuclei

E. Y. VILKOVISKIJ*†, R. V. E. LOVELACE‡, M. M. ROMANOVA‡,
L. A. PAVLOVA†, S. N. YEFIMOV† and E. B. BATURINA†

†Observatory, Fesenkov Astrophysical Institute, 050020 Almaty, Kazakhstan
‡Cornell University, Ithaca, New York 14853, USA

(Received 20 October 2005)

We consider the physical properties of matter outflow from active galactic nuclei in a unification model. The unification model of the outflow assumes that the source of the absorbing matter is the internal surface of the obscuring torus, and the model includes two-phase gas dynamics, radiation transfer and absorption spectrum calculations in the ultraviolet and X-ray bands. We analyse the radial dependences of ionization, radiation pressure and absorption features on the model input parameters. We briefly discuss several questions about the mass source of the flow, its covering factors, the nature of narrow absorption details and others.

Keywords: Galactic nuclei; Broad-absorption-line quasars; Outflow; Model

1. Introduction

Matter outflow from active galactic nuclei (AGNs) have been detected owing to absorption details, visible mostly in the ultraviolet (UV) and X-ray bands. The broad-absorption-line (BAL) quasistellar objects (QSOs) (in the following, the usual term quasars is used, which is a contraction of this) were discovered at the end of the 1960s [1, 2] and attracted increasing attention from the beginning of the 1980s [3–5]. The intrinsic UV absorptions in BAL quasars are observable in optics with ground-based telescopes owing to large red shifts of the objects with $z \approx 2$.

Later the rapid development of cosmic telescopes for UV and X-ray bands provided many new results, including precise spectral observations of absorptions in the UV and X-ray spectra of Seyfert galaxies and quasars [6–13]. Now the amount of data regarding outflows from AGN is rapidly increasing, but still there is no commonly accepted theory that can implicitly describe the spectra, physical properties, geometry and dynamics of the absorbing flows. As a result, empirical models and different empirical interpretations of observed properties of the outflows have predominated in the last few years.

*Corresponding author. Email: vilk@aphi.kz

Astronomical and Astrophysical Transactions
ISSN 1055-6796 print/ISSN 1476-3540 online
http://www.tandf.co.uk/journals
DOI: 10.1080/10556790500487122

The earliest models of matter outflows from AGNs used different approaches to the outflow dynamics, including discussions of drag forces and cosmic rays in a two-phase medium [14, 15] and a thermal wind from the accretion disc [16]. Most of the following dynamic models considered mainly the radiation pressure force. Scoville and Norman [17] suggested that quasar BALs originate in stellar contrails driven by radiation pressure acting on dusty gas. Arav *et al.* [18] considered radial outflows of clouds, driven by radiation pressure in spectral lines by analogy with the hot-star wind theory [19]; the models proposed by Murray and Chang [20, 21] and Proga *et al.* [22] used the same forces to describe the flows along the accretion disc surface. Although the models can produce some absorption lines, the calculated spectra are very different from the observed spectra, and many questions about the structure and physics of the flow remains unanswered. In the last few years, some empirical models have been proposed [23, 24]. Unfortunately, none of these models solved the main problems of the AGN outflows.

Among the most important problems, we should mention the source of the absorbing matter, its characteristic distances from the AGN centrum, the main forces which determine the dynamics of the absorbers, and the problem of the confinement of the absorbing cloudlet. Possible sources of the absorbing matter could be the surface of the accretion disc, the internal surface of the obscuring torus, and the stellar contrails driven by drag forces of the environment and by radiation pressure. Also, any clouds that wandered into the line of sight can add its absorption details to the spectrum of the AGN. For instance, the analysis of the NGC 4151 absorptions by Kraemer *et al.* [25] showed that several absorption details visible in the spectrum belong to the absorbing 'clouds' spread form a distance $R = 0.03$ pc to a distance $R = 2150$ pc. The question is: can all these absorbers be described as belonging to a common outflow? In principle, it is possible that several sources of absorption with different dynamics (say, gas clouds starting from the accretion disc, from the obscuring torus and from the starburst) can contribute to the spectrum of a particular object, which makes any theoretical analysis difficult. Taking into account these complications, it is reasonable to start with a 'pure' case, and we choose BAL quasars as a homogeneous subclass.

In the present paper, we consider the 'unification outflow model' which is based on the standard unification model of AGNs [26] and define the internal surface of the obscuring torus as the main source of the absorbing matter. The physical grounds and properties of our model were presented in [27]. Here we shall discuss the model in more detail, considering the radial behaviour of physical properties of the outflow, which depends on the input parameters of the model.

The structure of the paper is as follows: in section 2 we discuss the main physical components of the model; in section 3 we recall some approaches to the model calculation; in section 4 we consider some model solutions and discuss the behaviour of the physical properties of the outflow; our conclusions are presented in section 5.

2. The main physical components of the model

Although we suppose (as is widely accepted) that the geometrical unification scheme is valid for both Seyfert galaxies and quasars, we cannot be *a priori* positive that the dynamic models of the matter outflow should be the same in both cases. The observed properties of matter outflows are different in these subclasses. The main difference is the wideness of the absorption details, which points to a larger characteristic outflow velocities in BAL quasars than in Seyfert galaxies. In the former case there are many objects with the outflow velocities as high as 5000 km s^{-1} and many of these have velocities as much as several tens of kilometres per second (for comments about the narrow absorptions in quasars, see below), while in the last case the outflow velocities are typically less then $2000\,\mathrm{km\ s^{-1}}$. It should be noted, however, that many quasars (50%) have in the spectra only narrow 'associated' absorption details with velocities less than $5000\,\mathrm{km\ s^{-1}}$, quite similar to those of the absorption of Seyfert galaxies; these objects will be discussed below.

There are also differences in the fraction F of objects with absorbing outflows among all objects of the two subclasses (quasars and Seyfert galaxies). In the unification paradigm this fraction is closely related to the global covering factor of the outflow, $C_{\mathrm{g}} = F\bar{C}_{\mathrm{f}}$, where $\bar{C}_{\mathrm{f}} \approx 1$ is the average covering factor among the objects with absorption. The quasars with BALs in their spectra represent about 12–15% (the apparent fraction) of all the optically detected quasars [4, 28]. Taking into account the role of the K correction in flux-limited samples, the 'real' fraction of BAL quasars can be estimated as $F \approx$ 20–25% [29]. In the framework of the geometrical unification scheme the explanation is that almost all (at least all radio-quiet) quasars contain non-spherical absorbing outflows with the global covering factor close to the 'real' quasar fraction. In Seyfert galaxies the correspondingly defined factor F is estimated to be much larger, up to $F \approx$ 60–70% [7, 30], but it includes all objects with absorptions and is not separated by their dependence on the linewidth.

As noted above, many quasars ($F \approx 50\%$) have in their spectra only 'narrow' absorption details with a velocity shift $\Delta v < 5000\,\mathrm{km\,s^{-1}}$, which were called 'associated absorptions', quite similar to the absorption of Seyfert galaxies. Ganguly *et al.* [31] found that $F = 0.25$ for the associatd absorptions in the C IV line of $z < 1$ quasars; however, Laor and Brandt [32] found that $F = 0.5$ for $z < 0.5$ quasars, and Vestertgaard [33] obtained $F = 0.55$ for quasars in $1.5 < z < 3.5$. If we unify all quasars with any absorption lines into a common group, we obtain the result that the 'total' F is about 0.6–0.7 and that the values are approximately the same for quasars and Seyfert galaxies. However, in our opinion, this statement has to be considered with great caution for the following reasons.

(i) A sufficient number of these associated absorptions are not intrinsic but intervening [32].
(ii) Roughly equal parts (about 0.5) of the radio-quiet and radio-loud quasars show narrow UV absorption lines [33] with stronger lines among the lobe-dominated radio-loud quasars.

In our opinion, the last result shows that many of the associated absorptions in quasars can present a principally different case of outflows and, in particular, those related to the starburst events rather than to 'pure' AGN outflow; the same restrictions can be, in principle, valid for some Seyfert absorptions.

Because of this, we concentrate here on one particular subclass of AGNs, the BAL quasars. The broad blue absorption lines of BAL quasars, in contrast with the classical P Cygny profiles, is not accompanied by emission in the red part of the line profile, which is naturally explained by the non-spherical geometry of the BAL quasar outflows. The BALs seen in the quasar spectra originate not in the outflow but in the much more compact region (broad-emission-line region) close to the accretion disc, which, as a rule, is shielded by the outflowing gas.

The emission spectra of BAL quasars are similar to those of non-BAL quasars [34, 35], but the BAL quasars are mostly radio-quiet objects [36]. The evidence of the so-called line-locking effect [37–39] is a notable peculiarity of many BAL spectra. This effect indicates the essential influence of the radiation pressure in the spectral lines on the gas dynamics. Understanding the physics of this particular subclass of AGNs is extremely important for understanding the physics of AGNs as a whole [4, 40, 41].

We choose the geometry of the model proceeding from the standard unification scheme, including the obscuring torus as a main element. The second important element of our model is the hot-gas outflow, which starts from the outer surface of the accretion disc and fills in the internal hole of the obscuring torus. We assumed that the main source of the absorbing matter of the outflow (producing the blue-shifted absorption lines) is the flow of clouds of the cold gas, which starts at the inner surface of the obscuring torus and then is involved in the outflow of a hot gas. This structure of the outflow has been confirmed in recent work [42, 43].

Let us discuss the physical components of the two-phase outflow in more detail.

2.1 *The hot-gas outflow*

The presence of the hot corona above the accretion disc (with temperatures up to 10^8–10^9 K) follows from the common presence of X-ray radiation in the AGN spectra with a spectral energy distribution close to $F(E) \propto E^{-\alpha}$ with $\alpha \approx 2$. Modern theoretical models involve a hot corona to explain the continuous emission distribution mainly by Comptonization of the thermal radiation of the 'cold' accretion disc [44–49].

On the other hand, not only the outflows from hot corona but also the gas evaporation from the inner shell of the obscuring torus and heated by the AGN radiation, by the jet [50] and by the strong shocks and cosmic ray outflow from the AGN variable 'machine' will create the hot gas that fills in the hole of the obscuring torus and outflows owing to the hot-gas pressure. At the border of the hot gas and the cold dusty gas of the obscuring torus the Rayleigh–Taylor instability will produce a transition layer consisting of both hot-gas and cold-gas elements, i.e. it is a multiphase medium, which moves under the action of radiation pressure and mutual drag forces. The presence of the two-phase medium in AGNs follows from the analysis of stability of the astrophysical plasma in the radiation field of AGNs [51, 52]. In any case, the cloudy structure of the 'cold' absorbing clouds requires the presence of the intercloud confining 'hot' medium.

Proofs of the existence of the hot plasma (outside the accretion disc corona) can be very difficult to obtain by a straightforward observational method. The presence of the hot gas in the continuum can appear as free–free radiation with the total power equal to $L_{\mathrm{ff}} = 1.5 \times 10^{-27} T^{1/2} (\mathrm{EM_h})\,\mathrm{erg\,s^{-1}}$, where $\mathrm{EM_h} = n_e^2 V$ is the emission measure of the hot gas, n_e is electron density and V is the volume of the hot gas. If we suppose that $n_e \approx 10^4\,\mathrm{cm}^{-3}$, $T_e \approx 10^8$ and $V \approx 3.4 \times 10^{56}\,\mathrm{cm}^3$ (close to a cubic parsec), we have $\mathrm{EM_h} \approx 3.4 \times 10^{64}\,\mathrm{cm}^{-3}$ and $L_{\mathrm{ff}} \approx 5 \times 10^{41}\,\mathrm{erg\,s^{-1}}$, which is much less than the typical quasar X-ray luminosity ($L_X \approx 10^{44}\,\mathrm{erg\,s^{-1}}$). More straightforward evidence can be obtained from the highly ionized lines of heavy elements such as the Fe XXVI Lyman-α line. Now such data have started to be obtained, but still the interpretation of the observational data is controversial. The observational signs of the high-ionization species of many elements were provided by the present-generation X-ray missions XMM-Newton and Chandra, which revealed new features in the spectra of AGNs. Both the emission lines from Fe XXV and Fe XXVI ions [53, 54] and the absorption lines of Fe XXV and Fe XXVI ions [55–58] were observed. The interpretation of the data [53, 59, 60] is in agreement with the orientation-dependent unification model with a wide distribution of temperatures of the ionized gas, up to $T \approx 10^6$–10^7 K. These data are related to Seyfert galaxies; there are no observational data regarding the presence of the hot gas with $T \approx 10^8$ K in quasars, which is the task for the next-generation X-ray telescopes.

2.2 *The compact stellar cluster*

The next physical subsystem postulated in [27] is a compact and massive stellar cluster with a characteristic size close to the size of the obscuring tori. Now the first evidence of a compact stellar cluster (CSC) in AGNs was provided by recent observations of the structure of AGNs on a 0.1 s resolution scale [61, 62]. Also the reality of a supposed CSC in an AGN can be seen also in 'relict' clusters frequently observed in the centres of 'quiet' galaxies containing a supermassive black hole [63] and the stellar clusters in the centres of late-type galaxies [64].

The modern models of the obscuring tori [65, 66] suppose that the gas matter of the dusty tori is ejected from stars of the CSC with a characteristic radius less than 100 pc and a mass larger then $10^9 M_{\odot}$.

The evolution of an AGN is driven mainly by intergalactic interaction and merging (see, for example, [67, 68] and references therein). Every merging event leads to a new 'duty cycle' of the AGN activity, accompanied by a starburst event in the earlier stages. The first phase of the cycle starts with the creation of a new CSC by a power starburst in the massive dense gas cocoon around the massive black hole. The gas and stars in the centre of the cocoon have a specific angular momentum and therefore create a new accretion disc around the central masssive black hole. At the end of this phase, the polar gas outflows and jets produce polar holes in the cocoon along the symmetry axis, transforming it to a typical 'obscuring torus'. Then the bright AGN phase starts, lasting about 10^7–10^8 years. In this bright phase of the AGN's duty cycle, the masses of the CSC and obscuring torus gradually decrease, leading to the third phase with diminishing activity corresponding to weak Seyfert nuclei and low-ionization nuclear emission-line regions. This evolution sequence of obscuring tori during a duty cycle is remarkably similar to the evolution scheme derived from observations of the infrared (IR) spectra of AGNs by Haas *et al.* [69].

2.3 *The flow of the obscuring clouds*

We suppose that the main source of the obscuring matter is the cold gas in the internal surface of the obscuring torus. Both the Rayleigh – Taylor instability due to the radiation pressure and the Kelvin – Helmholtz instability due to the velocity shear at the border of the hot and cold gases lead to the creation of cold clouds embedded in the hot flow. The hot gas provides confinement of the cold clouds; the large clouds will divide into smaller clouds, and the smallest clouds will evaporate and finally will probably disappear. As a result, the maximum absorption will be provided with cloudlets of some intermediate masses. The real kinetics leading to the true distribution function of the cloud masses can be complicated; below we choose some 'characteristic' mass of the clouds in the model, taking into account the possibilities that the line-locking effect appears and that the calculated and observed spectra are similar.

3. Radiation pressure and gas dynamics

In the general case we must solve the radiation hydrodynamics equation system, including the mass continuity equation, the momentum and the energy equations for both the gas flows and the radiation transfer equations for both the continuum and the lines. The equation system is obtained from the photoionization balance equations for the clouds and the hot gas. The equations depend on the central object mass, luminosity and spectrum, and on the CSC parameters.

To calculate the radiation pressure force acting on a cloud, we first have to solve the photoionization task along the cloud to find the column densities of different ions. This task includes determination of the ionization radiation transfer equation and the system of equations for the ionization balance calculations, taking into account the collision ionization, photoionization and recombination, and the Auger effect and ionization from the internal electronic shells of ions. This task requires a fair amount of time; so in model simulations of the dynamic task we return to the photoionization task not in every step of the dynamic task, but with some larger steps, determined on the condition that the expected relative ion numbers change by several per cent.

Our theoretical approach to the problem is based on the assumption that similar dynamic processes are responsible for both the broad absorptions and the narrow details of the BAL quasar spectra; so the explanation of the last (more delicate) phenomenon permits us to solve the problem of the broad absorption as a whole. It was Milne [70] who predicted the change in the dynamics of the ions (atoms) accelerated by the radiation pressure due to the influence of the absorption lines. More than 40 years later, Scargle *et al.* [71] considered a similar effect due to the shift of the line to the continuum edges such as the Lyman edge. The same principle in the case of two lines was discussed by Mushotzky *et al.* [72], who call it the 'line-locking' effect. Of course, the line-locking effect features are observed in BAL quasar spectra, and the most impressive are in the spectrum of Q1303 + 308 [38].

The heat balance analysis of the two-phase medium situated in the central part of AGNs [51, 52] shows that the temperature of the hot gas is rather high, about 10^7–10^8 K. Because of this, the electron heat conductivity is high, and we may treat the stream of the hot gas as an isothermal flow as a first approximation. The position of the transonic point depends mostly on the relation of the compact stellar kernel mass to the mass of the black hole. It can be argued that the outer critical point at a distance about 1 pc is more preferable for the BAL quasar models. Physically this means that the hot-gas stream becomes supersonic at the distance of the obscuring torus, where the broad absorptions are formed. Of course, the isothermal flow of the hot gas is a first approximation only. There are several mechanisms of hot-gas heating; the most important seems to be bow shocks and energy dissipation of cosmic rays. As the details of the heating mechanism are still not known, the simplest approximation of the 'constant temperature gradient' is used. We supposed that the terminal velocity of clouds is connected with the hot-gas terminal velocity and, introducing a positive temperature gradient into the hot-gas flow equation, we have solutions with terminal velocities as high as (20–30)$\times 10^3$ km s^{-1}. The equation for the hot-gas dynamics has been presented in [27].

We suppose that the radiation transfer in the spectral lines is determined by the resonance scattering process in only the clouds, because the optical depth in the intercloud medium is very thin.

For a line we determine the optical depth of a cloud at the line centre as $\tau(\nu_i) = (\pi e^2/mc) N_i f_i / \Delta\nu_{\mathrm{D}}$, where e and m are the electronic charge and mass respectively, N_i is the cloud's column density of the ions which can absorb (scatter) the photons with the frequency υ_i, f_i is the oscillator strength and $\Delta\nu_{\mathrm{D}} = \nu_i \upsilon_{\mathrm{th}}/c$ is the turbulent Doppler width (υ_{th} and c are the ion turbulent velocity and the light velocity, respectively). Every cloud absorbs the $1 - \exp(-\tau_i)$ part of the radiation flow at a line centre, and the clouds can shield each other. Then we have the differential equation for the spectral density $\Phi(\upsilon)$ of the radiation flow:

$$\frac{\mathrm{d}\Phi(\upsilon)}{\mathrm{d}r} = -\Phi(\nu) N_{\mathrm{cl}} S_{\mathrm{cl}} \left\{ 1 - \exp\left[-\sum_i f(\nu - \nu_i)\tau(\nu_i) \right] \right\}, \tag{1}$$

where N_{cl} is the number of clouds in a volume unit and S_{cl} is the geometrical cross-section of a cloud (so $N_{\mathrm{cl}} S_{\mathrm{cl}}\, \mathrm{d}r$ is the probability that a photon meets a cloud at the distance dr); under the exponent there are the normalized line profile functions $f(\nu - \nu_i)$ and the optical depths $\tau(\nu_i)$ for the resonance scattering at the line centres in a cloud. The Doppler-shifted frequency is

$$\nu_i = \nu_{i0} \left(\frac{1 + V/c}{1 - V/c} \right)^{1/2} \approx \nu_{i0} \left(1 + \frac{V}{c} \right),$$

where V is the cloud's velocity and ν_{i0} is the central frequency of the appropriate ith line.

Therefore both the filling factor and the velocity of the clouds are taken into account; in the case of a finite length (when integrating over dr), this leads to the equation which was discussed in [73]. The equation of the ionizing radiation transfer can be written similarly [27].

The equation of motion of a separate cloud is

$$m_{\rm cl}\frac{{\rm d}V}{{\rm d}t} = F_{\rm lin} + F_{\rm cont} + F_{\rm drag} - F_{\rm gr}, \tag{2}$$

where $m_{\rm cl}$ is the cloud's mass and V its velocity; on the right-hand side there are the forces of the radiation pressure due to the scattering of the radiation by the ion lines, the forces of the radiation pressure due to continuum absorption, the drag force due to the difference between the velocities of the cloud and the hot-gas stream, and the gravitational force respectively.

From the numerical solutions we have calculated the radiation force acting on a cloud as the difference between the radiation flow moments before and after the cloud crossing:

$$F_{\rm rad} = F_{\rm lin} + F_{\rm cont} = \frac{S_{\rm cl}}{c\left[\int \Phi(\nu)h\nu\,{\rm d}\nu|_{\rm before} - \int \Phi(\nu)h\nu\,{\rm d}\nu|_{\rm after}\right]}.$$

We use the Gaussian profiles in the line-transfer equation (1) and, when solving the full equation system numerically, we take the cloud velocity differences from step to step be less than one fifth of the linewidths; this condition is necessary for correct calculations of the line-locking effect.

The drag force depends on the square of the velocity difference between the cloud and the hot gas: $F_{\rm drag} = \rho_{\rm hg}S_{\rm cl}[v(r) - V(r)]|v(r) - V(r)|$. For the spherical clouds, confined by the hot-gas pressure, $S_{\rm cl} = \pi\{m_{\rm cl}/[4/3\pi\rho_{\rm hg}(T_{\rm hg}\mu_{\rm cl})/(T_{\rm cl}\mu_{\rm hg})]\}^{2/3}$ from the pressure balance condition $(\rho_{\rm cl}/\mu_{{\rm cl}l})T_{\rm cl} = (\rho_{\rm hg}/\mu_{\rm hg})T_{\rm hg}$; here $\rho_{\rm cl}$, $T_{\rm cl}$ and $\mu_{\rm cl}$ are the mass density, the temperature and the molecular weight respectively of the cloud's gas and $\rho_{\rm hg}$, $T_{\rm hg}$ and $\mu_{\rm hg}$ are the corresponding values for the hot gas.

The numerical solutions of the full equation system described above were obtained under the following assumptions.

(i) We modelled the incoming continuum spectrum (before the absorption) of the central object as the sum of the Planck spectrum and the power-law spectrum.
(ii) We assume that the absorbing flow started at the radius $R_0 \approx 1$ pc, which is larger than the radius of the broad-emission-line region; so we add the broad emission line to the AGN continuum. As the spectrum of a quasar is not known definitely in the wavelength interval from about 900 to 200 Å, there is the problem of constructing the broad-line intensities in this band. Because of this we use two different templates for the emission-line intensity: one for the 'high-intensity' limit, and the other for the 'low-intensity' limit.
(iii) We introduce the flow of the absorbing clouds as a function of the radial distance from the central object, starting with very low flow at R_0, then increasing linearly along the radius and becoming constant (or dropping slowly) above some distance $R_{\rm max}$, which is assumed to be the upper border of the obscuring t orus.
(iv) At every step of the numerical solution we calculate the gas dynamics and the spectrum of the radiation flow. We took into account 237 strong-resonance lines of the most important ions.

4. The model calculation

Some preliminary results of the BAL quasar model calculations were presented in [27]. It was shown that the absorption in spectral lines has two main shapes: broad 'troughs' and a system of narrow lines, divided into regular intervals. The last type is known as the 'line-locking effect'. It was shown that the line-locking effect is simulated in the BAL quasar spectra owing to the 'quantization' of the cloud acceleration and the velocity on the 100 pc scale, and we concluded that the main reason for the velocity structure is the nonlinear interaction of the clouds, the hot gas and the radiation field. The stability of the line-locking effect in the variable BAL quasar q1303 + 308 was analysed by Vilkoviskij and Irwin [74], and it was shown that the structure of the line-locking effect is quite stable in the 20 year interval in spite of strong variations in the absorption depths of the narrow details. We pointed out the following conditions which promote the line-locking effect: the acceleration due to the line-scattered radiation must exceed the continuum absorption acceleration; so the masses of the clouds must be rather small, typically about 10^{-13}–10^{-15} of the solar masses. The mass flow of the clouds must be limited, typically close to $\Phi_{\rm cl} = q(10^{-1} - 10^{-3})M_\odot$ year^{-1}, where q is the 'global' covering factor (as seen from the central object). Now we shall consider the physical properties of the outflows in more details to investigate the reason for the appearance of line-locking (LIL) in our model. We choose the parameters of our model in such a way that the output spectrum, resulting in the model stimulation, is similar to the observed spectrum. For example, in the next two figures we show the observed and calculated spectra for two BAL quasars NGC 1314 and q1303 + 308 (the last with a strong line-locking effect). Then we investigated the radial dependences of physical properties of the outflows.

In figure 1 we show the spectra of the BAL quasar NGC 1314.

The most important parameters of the model are as follows. The mass of the black hole is $M_{\rm BH} = 1.3 \times 10^9 M_\odot$; the Planck spectrum luminosity is $L_{\rm Pl} = 5 \times 10^{46}$ergs^{-1}; the power spectrum luminosity (with $\alpha = 1.8$) is $L_{\rm p} = 1.5 \times 10^{46}$ergs^{-1}; the hot-gas flow is $F_{\rm h} = 0.05 M_\odot$year^{-1}; the cold cloud flow increases from $F_{\rm cl} = 0.001 M_\odot$year^{-1} at $r = 0.1$ pc to $F_{\rm cl} = 0.01 M_\odot$year^{-1} at $r = 2$ pc and to $F_{\rm cl} = 0.15 M_\odot$year^{-1} at $r = 4$ pc. The mass of one

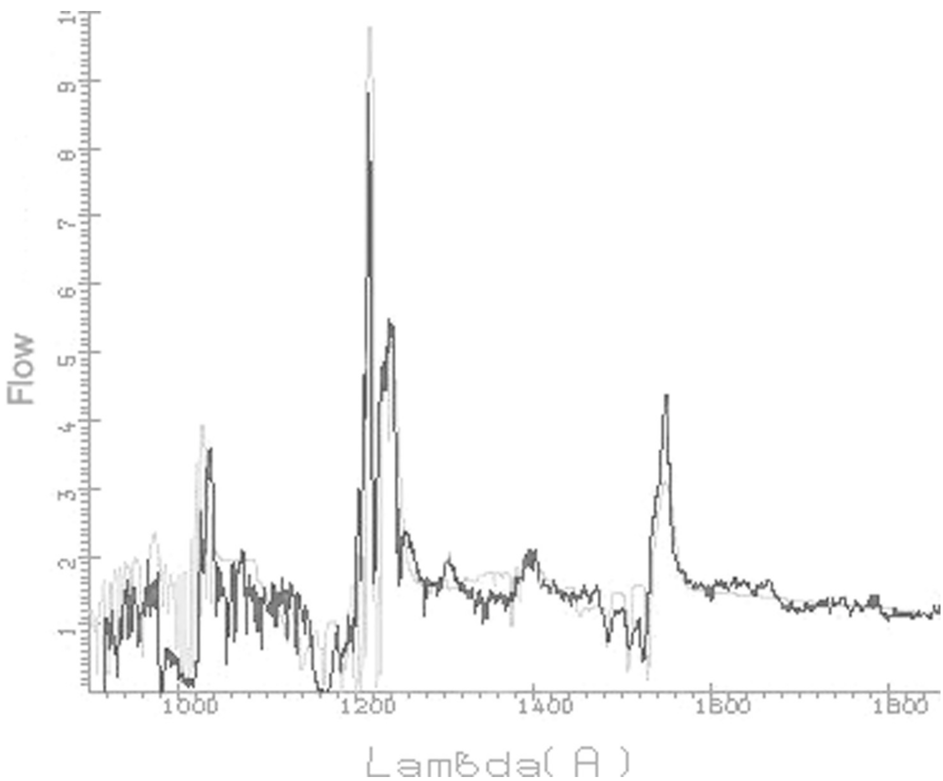

Figure 1. The calculated (faint line) and observed spectra of NGC 1314.

cloud is $M_{cl} = 5 \times 10^{-14} M_{\odot}$, its temperature is $T_{cl} = 10^3$ K and the turbulent velocity is $V_T = 2.8 \times 10^7$ km s^{-1}. The relative amplitude of the $L\alpha$ broad emission line to the continuum is 5.5.

The radial dependences of some parameters are shown in the next few figures for the quasar q1303 + 308.

The comparison of the observed and calculated spectra is presented in figure 2; one can see that the calculated spectrum is similar to the observed spectrum with respect to the line locking and also its velocity structure.

The main parameters of the model are $M_{BH} = 1.3 \times 10^9 M_{\odot}$, $L_{Pl} = 15 \times 10^{46}$ergs^{-1} and $L_p = 2 \times 10^{46}$ergs^{-1}, with = 1.7; $F_h = 0.05 M_{\odot}$year^{-1}; the absorbing flow increases from $F_{cl} = 0.001 M_{\odot}$year^{-1} at $r = 0.1$ pc to $F_{cl} = 0.007 M_{\odot}$year^{-1} at $r = 2$ pc and to $F_{cl} = 0.4 M_{\odot}$year^{-1} at $r = 8$ pc. The mass of one cloud is $M_{cl} = 5 \times 10^{-16} M_{\odot}$, its temperature is $T_{cl} = 10^3$ K and the turbulent velocity is $V_T = 1.6 \times 10^7$ km s^{-1}. The relative amplitude of the $L\alpha$ broad emission line with respect to the continuum is 1.5.

One can see that the main differences between the model parameters for the two objects are the Planck temperature, the masses of the absorbing clouds and the emission lines with respect to the continuum relative intensities.

The radial dependence of the cold cloud's velocity for q1303 + 308 is presented in figure 3; one can see that the velocity has a 'ladder' structure, which provides the line-locking effect in the spectrum.

In figure 4, we show the radial behaviours of several carbon ions for our solution; for comparison, in figure 5 we plot the same dependences for the case of very thin cold-gas outflow $F_{cl} = 10^{-6} M_{\odot}$year^{-1}; one can see the absorption of the ionizing continuum by the real outflow (figure 4) change in the relative ion quantities.

In figure 6, we plot the velocity dependences of the radiation pressure forces acting on several ions in comparison with the total radiation pressure force in the model solution for

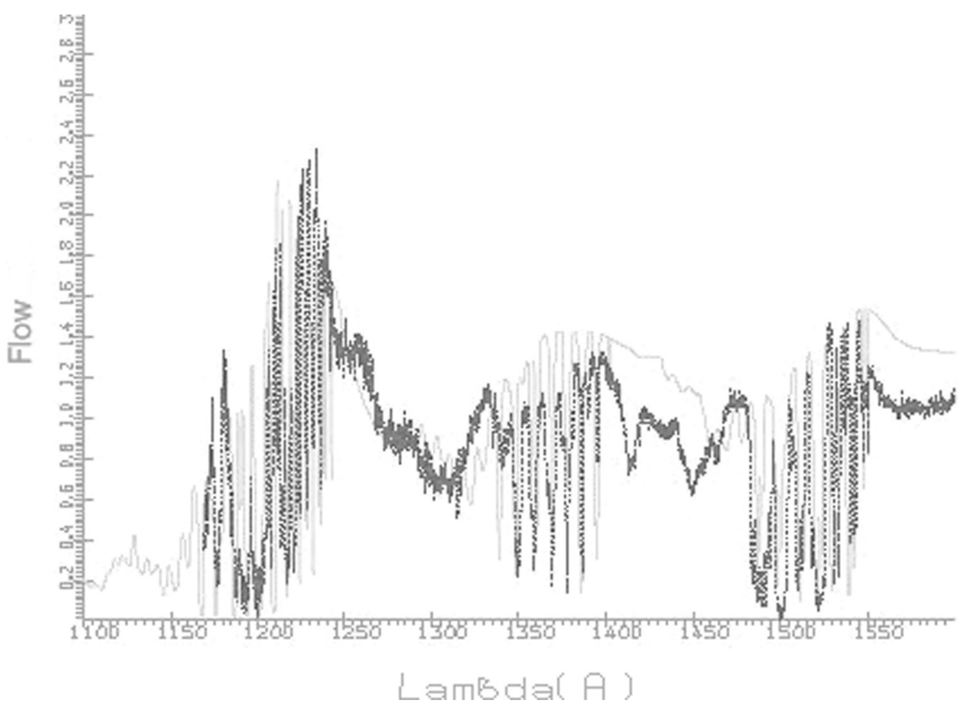

Figure 2. The calculated (faint line) and observed spectra of q1303 + 308.

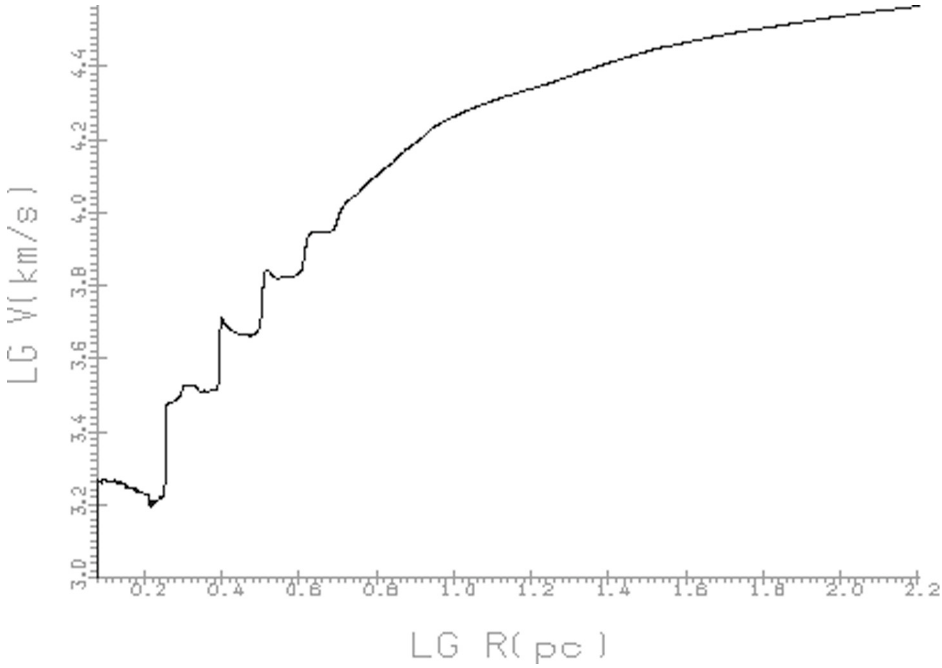

Figure 3. The behavior of velocity of absorbing matter depending on distance.

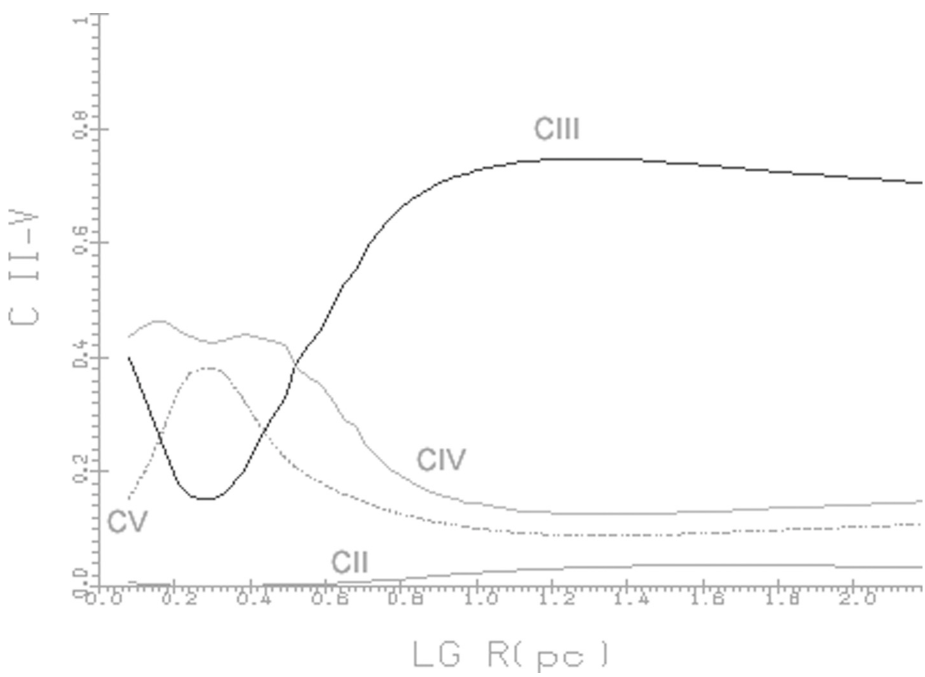

Figure 4. The relative number of C-ions depending on distance.

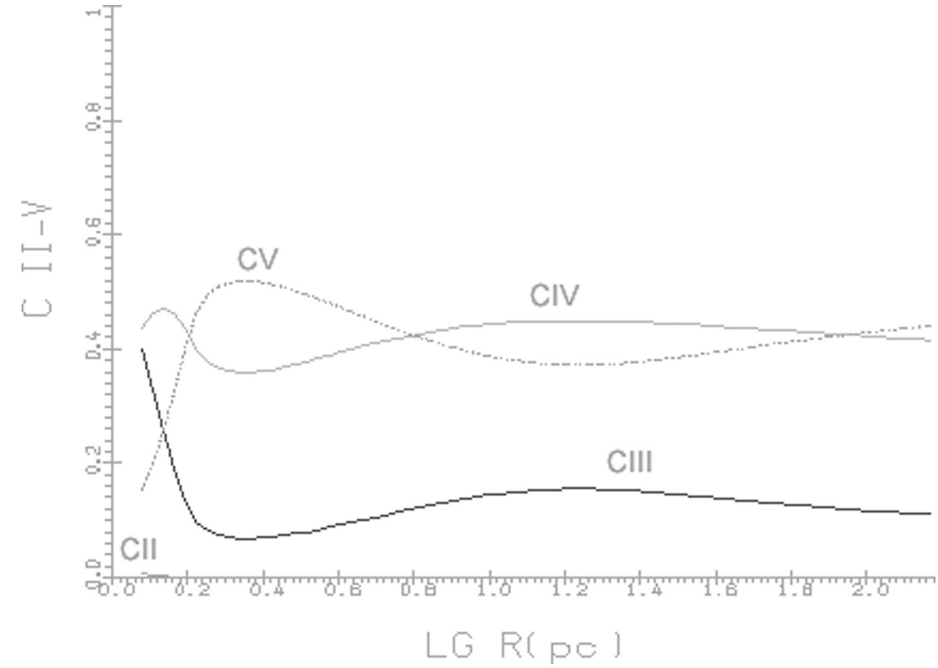

Figure 5. The relative number of C-ions depending on distance in the very thin flow.

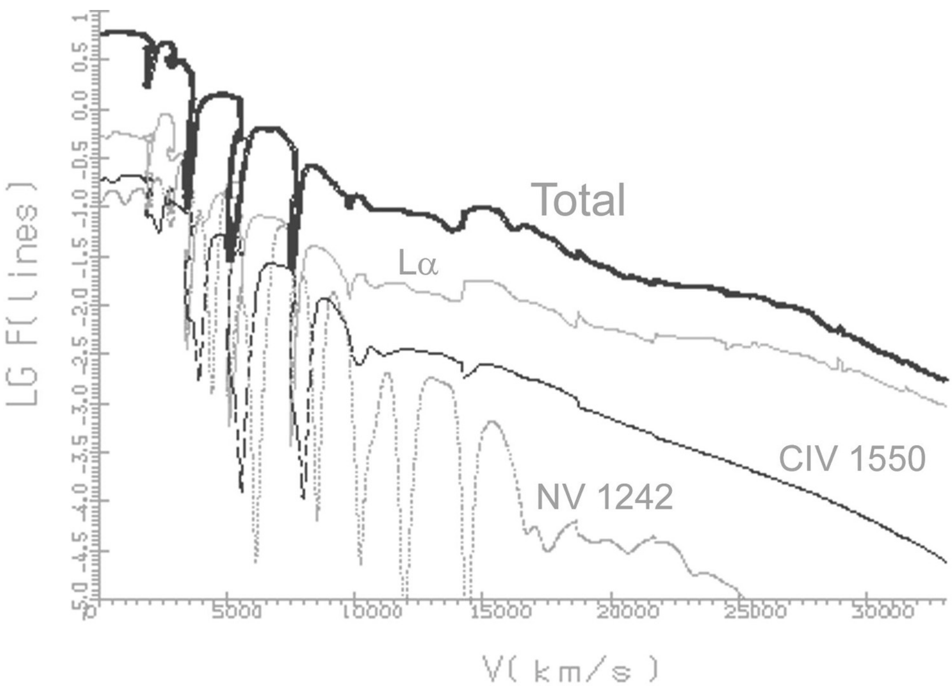

Figure 6. The radial dependence of the radiation pressure forces in q1303 + 308.

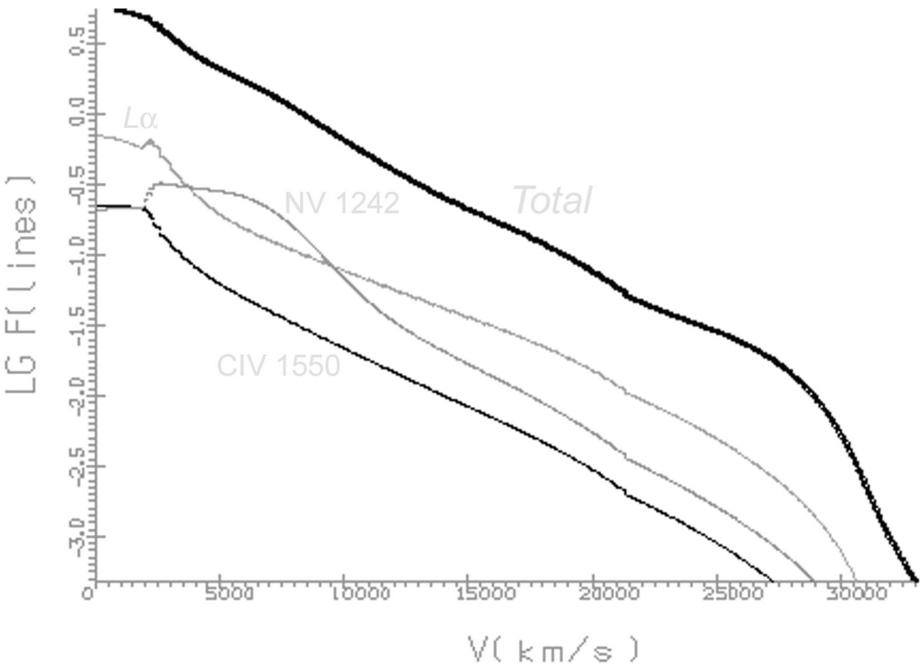

Figure 7. The radial dependence of the radiation pressure forces in a very thin flow.

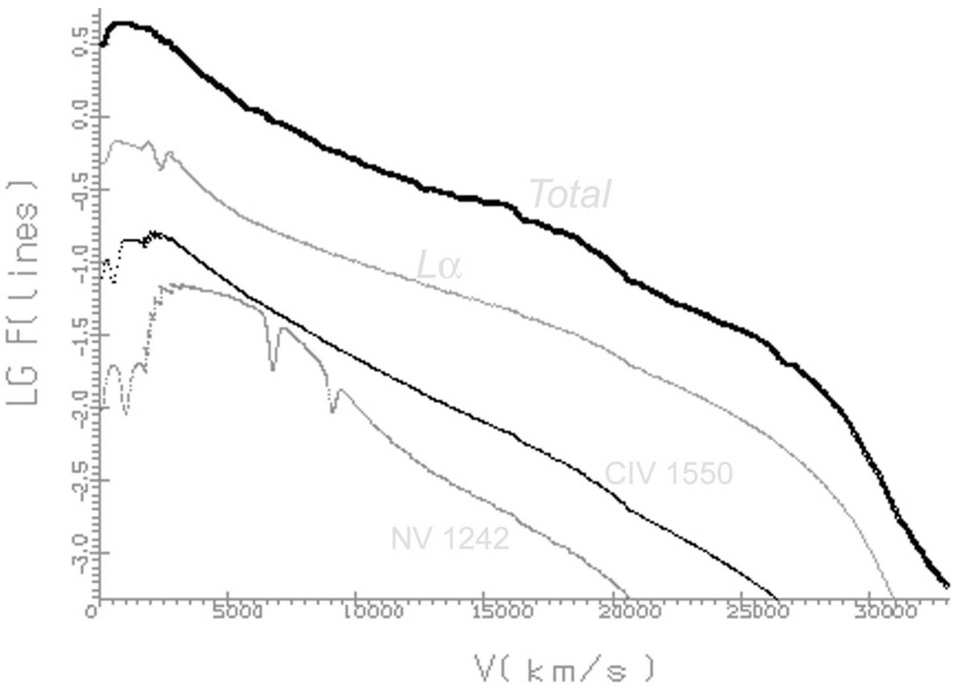

Figure 8. The radial dependence of the radiation pressure forces with an absorbing cloud in the base of the flow.

q1303 + 308. One can see the strong non-monotonic dependences due to absorptions in the clouds with almost constant velocities in the ladder-like structure of the flow.

For comparison, in figure 7 we plot the same dependences for the case of 'thin' flow ($F_{\rm cl} = 10^{-6} M_{\odot}\text{year}^{-1}$) and in figure 8 the case of the same small flow, but with an absorbing cloud ($N \approx 10^{22}\,\text{cm}^{-2}$) at the beginning of the outflow. One can see that the 'troughs' in the total radiation force due to the absorptions by the cloud at the base of the flow are usually insufficient for initiation of the line-locking effect; so the nonlinear processes of two-phase radiation dynamics play the most important role in the line-locking effect.

5. Conclusions

The similarity of the calculated spectra to the observed spectra in itself is not decisive proof of the model; in particular, it is possible (in principle) that some 'scaling' of the model parameters could leave the resulting spectrum almost unchanged. Nevertheless, in our opinion, the similarity of the observed and calculated features of the line-locking effect in the quasar q1303 + 308 confirms that our model represents the main nature of the outflow in a proper way.

In particular, the relative depths of the two components of the same doublet lines (as in the cases of the C IV and Si IV doublets; the N V case is not so evident here) show that the 'covering factor' is reproduced well in our model, even if the parameters of the clouds (such as the temperature and the turbulent width) are assumed to be unchanged with distance. We recall that in our model the 'covering factor' at a specific velocity means the relative area of the source of the continuum radiation, which is shadowed by the cloud's projections in a velocity interval equal to the turbulent velocity in the cloud. However, we stress that the shape of the troughs produced by the doublet intensities and by overlapping depends on the 'velocity profile' of the ladder-like velocity structure, where reverse velocities (deceleration) are possible. It is possible that nonlinear dynamic effects, leading to non-monotonic acceleration of the absorbing matter and to the appearance of stable narrow details in the absorption spectra, are rather common in the outflows from AGNs. One of the important problems, which needs more analysis and determination of the physical basis, is the characteristic size (mass) of the absorbing clouds in the two-phase outflow.

Further investigation of the model solutions in comparison with the observed spectra, including absorption lines in the X-ray band, are needed for more definite conclusions about the physical nature of the absorbing matter outflows from AGNs.

Acknowledgement

We are grateful to the US Civilian Research and Development Foundation (grant PQ2-2555-AL-3) for supporting this work.

References

[1] C.R. Lynds, Astrophys. J. **147** 396 (1967).
[2] E.M. Burbidge, Astrophys. J. Lett. **160** L33 (1970).
[3] R.J. Weymann, R.F. Carswell and M.G. Smith, A. Rev. Astron. Astrophys. **19** 41 (1981).
[4] D.A. Turnshek, in *QSO Absorption Lines: Probing the Universe*, Space Telescope Science Institute Symposium Series, Vol. 2, edited by J.C. Blades, D.A. Turnshek and C. Norman (Cambridge University Press, Cambridge, 1987), p. 17.
[5] R.J. Weymann, C.B. Foltz and P.C. Hewett, Astrophys. J. **373** 23 (1991).
[6] S.B. Kraemer, D.M. Crenshaw, J.B. Hutchings, I.M. George and A.C. Danks, Astrophys. J. 671 (2001).
[7] C.S. Reynolds, Mon. Not. R. Astron. Soc. **286** 513 (1997).

[8] I.M. George, T.J. Turner, R. Mushotzky, K. Nandra and H. Netzer, Astrophys. J. **503** 174 (1998).
[9] G.A. Kriss, A.F. Davidsen, W. Zheng, J.W. Kruk and B.R. Espey, Astrophys. J. **454** L7 (1995).
[10] G.A. Kriss, B.R. Espey, J.H. Krolik, Z. Tsvetanov, W. Zheng and A.F. Davidsen, Astrophys. J. **467** 622 (1996).
[11] D.M. Crenshaw, S.P. Maran and R.F. Mushotzky, Astrophys. J. **496** 749 (1998).
[12] J.S. Kaastra, R. Mewe, D.A. Liedahl, S. Komossa and A.C. Brinkman, Astron. Astrophys. **354** L83 (2000).
[13] S. Kaspi, W.N. Brandt, H. Netzer, R. Sambruna, G. Chartas, G.P. Garmire and J.A. Nousek, Astrophys. J. **535** L17 (2000).
[14] R.J. Weymann, J.S. Scott, A.V.R. Schiano and W.A. Christiansen, Astrophys. J. **262** 497 (1982).
[15] M.C. Begelman, M. de Kool and M. Sikora, Astrophys. J. **382** 416B (1991).
[16] M.C. Begelman, C.F. McKee and G.A. Shields, Astrophys. J. **271** 70 (1983).
[17] N. Scoville and C. Norman, Astrophys. J. **451** 510 (1995).
[18] N. Arav, Z.-Y. Li and M.C. Begelman, Astrophys. J. **432** 62 (1994).
[19] J. Castor, D. Abbot and R. Klein, Astrophys. J. **195** 157 (1975).
[20] N. Murray and J. Chang, Astrophys. J. **454** 105 (1995).
[21] N. Murray and J. Chang, Astrophys. J. **494** 125 (1998).
[22] D. Proga, J.M. Stone and T.R. Kallman, Astrophys. J. **543** 686 (2000).
[23] M. Elvis, Astrophys. J. **545** 63 (2000).
[24] G. Canalizo and A. Stockton, Astrophys. J. **555** 719 (2001).
[25] S.B. Kraemer, D.M. Crenshaw and J.R. Gabel, Astrophys. J. **557** 30 (2001).
[26] R. Antonucci, A. Rev. Astron. Astrophys. **31** 473 (1993).
[27] E.Y. Vilkoviskij, S.N. Efimov, O.G. Karpova and L. Pavlova, Mon. Not. R. Astron. Soc. **309** 80 (1999).
[28] D.A. Turnshek, Astrophys. J. **280** 51 (1984).
[29] P.C. Hewett and C.B. Foltz, Astrophys. J. **125** 1784 (2003).
[30] D.M. Crenshaw, S.B. Kraemer, A. Bogges, P. Stephen, R.F. Mushotzky and C.-C. Wu, Astrophys. J. **516** 750 (1999).
[31] R. Ganguly, N.A. Bond, J.C. Charlton, M. Eracleous, W.N. Brandt and C.W. Churchill, Astrophys. J. **549** 133 (2001).
[32] A. Laor, W.N. Brandt, Astrophys. J. **569** 641 (2002).
[33] M. Vestertgaard, Astrophys. J. **599** 116 (2003).
[34] V.T. Junkkarinen, E.M. Burbidge and H.E. Smith, Astrophys. J. **317** 460 (1987).
[35] C.C. Steidel and W.L.W. Sargent, Astrophys. J. **382** 433 (1991).
[36] J.T. Stocke and C.B. Foltz, Astrophys. J. **396** 487 (1992).
[37] J.D. Scargle, Astrophys. J. **179** 705 (1973).
[38] C.B. Foltz, R.J. Weymann, S.L. Morris and D.A. Turnshek, Astrophys. J. **317** 450 (1987).
[39] K.T. Korista, G.M. Voit, S.L. Morris and R.J. Weymann, Astrophys. J., Suppl. Ser. **88** 357 (1993).
[40] R.J. Weymann, D.A. Turnshek and W.A. Christiansen, in *Astrophysics of Active Galaxies and Quasi-stellar Objects*, edited by J. Miller (Oxford University Press, Oxford, 1985), p. 333.
[41] D.A. Turnshek, C.B. Foltz, C.J. Grillmair and R.J. Weymann, Astrophys. J. **325** 651 (1988).
[42] J.H. Krolik and G.A. Kriss, Astrophys. J. **561** 684 (2001).
[43] A.J. Blustin, M.J. Page, V. Fuerst, G. Branduardi-Raymont and E.C. Ashton, Astron. Astrophys. **431** 111 (2005).
[44] J. Chiang, Astrophys. J. **572** 79 (2002).
[45] A. Zadaziarski, J. Poutanen and W.N. Jonson, Astrophys. J. **542** 703 (2000).
[46] A. Rozanska and B. Cherny, Astron. Astrophys. **360** 1170 (2000).
[47] T. Kawaguchi, T. Shimura and S. Mineshige, Astrophys. J. **546** 966 (2001).
[48] M.A. Sobolewska, A. Siemiginowska and P.T. Zycki, Astrophys. J. **608** 80 (2004).
[49] J. Chiang and O. Blaes, Astrophys. J. **586** 97 (2003).
[50] S.Yu. Sazonov and R.A. Sunyaev, Astron. Lett. **27** 481 (2001).
[51] J.H. Krolik, C.F. McKee and C.B. Tarter, Astrophys. J. **249** 422 (1981).
[52] J.H. Krolik and G.A. Kriss, Astrophys. J. **447** 512 (1995).
[53] S. Bianchi, G. Matt, I. Balestra, M. Guainazzi and G.C. Perola, Astron. Astrophys. **422** 65 (2004).
[54] G. Matt, S. Bianchi, M. Guainazzi and S. Molendi, Astron. Astrophys. **414** 155 (2004).
[55] S. Kaspi, W.N. Brandt, I.M. George and H. Netzer, D.M. Crenshaw, Astrophys. J. **574** 643 (2002).
[56] J.N. Reeves, P.T. O'Brein and M.J. Ward, Astrophys. J. **593** L65 (2003).
[57] G. Matt, S. Bianchi, F. D'Ammando and A. Martoccia, Astron. Astrophys. **421** 473 (2004).
[58] J.N. Reeves, K. Nandra, I.M. George, K.A. Pounds, T.J. Turner and T. Yaqoob, Astrophys. J. **602** 648 (2004).
[59] S. Bianchi and G. Matt, Astron. Astrophys. **387** 76 (2002).
[60] S. Bianchi, G. Matt, F. Nicastro, D. Porquet and J. Dubau, Mon. Not. R. Astron. Soc. **357** 599 (2005).
[61] R.S. Davies, L.J. Tacconi and R. Genzel, Astrophys. J. **602** 148 (2004).
[62] R.I. Davies, L.J. Tacconi and R. Genzel, Astrophys. J. **613** 681 (2004).
[63] J. Kormendy, Rev. Mex. Astron. Astrofis. **10** 69 (2001).
[64] T. Boker, M. Sarzi, D. McLaughlin, R.P. van der Marel, H-W. Rix, L.C. Ho and J.C. Shields, Astron. J. **127** 105 (2004).
[65] M. Schartmann, K. Meisenheimer, M. Kamenzind, S. Wolf and T. Henning, Am. Inst. Phys. Conf. Proc. **761** 277 (2005).
[66] M. Schartmann, K. Meisenheimer, M. Kamenzind, S. Wolf and T. Henning, Astron. Astrophys. **437** 861 (2005).
[67] D.B. Sanders, B.T. Soifer, J.H. Elias, G. Neugebauer and K. Mathews, Astrophys. J. **328** L35 (1988).

[68] N. Mency, A. Cavalierre, A. Fontana, E. Giallongo, F. Poli and V. Vittoini, Astrophys. J. **587** L63 (2003).
[69] M. Haas, U. Klaas, A.H. Muller, F. Bertoldi, M. Camenzind, R. Chini, O. Krause, D. Lemke, K. Meinsenheimer, P.J. Richards and B.J. Wilkes, Astron. Astrophys. **402** 87 (2003).
[70] E.A. Milne, Mon. Not. R. Astron. Soc. **86** 459 (1926).
[71] J.D. Scargle, L.J. Caroff and P.D. Noerdlinger, Astrophys. J. Lett. **161** L115 (1970).
[72] R.F. Mushotzky, P.R. Solomon and P.A. Strittmatter, Astrophys. J. **174** 7 (1972).
[73] J. Kwan, Astrophys. J. **353** 123 (1990).
[74] E.Y. Vilkoviskij and M.J. Irvin, Mon. Not. R. Astron. Soc. **321** 4 (2001).